Washington University in St. I Louis Research

The following report from Washingtoon University for the period September-December 1995 contains the following brief chapters: :

1. Introduction
2. Review of Measurement Methodsls (Task 1)
3. Interpretation of Tracer Runs at LLaPorte (Task 4/Task 6)
4. Modification of CARPT-CT Systetem for Slurry Bubble Column Studies (Task 3)
5. Phenomenological Model for Liququid Recirculation (Task 3)
6. CTDLIB Codes and Simulation (Task 3)
7. References

Slurry Bubblle Column Hydrodynamics

Third Quarterly Repoort for Contract DOE-FC 22-95 PC 95051

Septeember - December, 1995

1 Introduction

The main goal of the subcontract t to the Chemical Reaction Engineering Laboratory (CREL) at Washington University is to studdy the fluid dynamics of slurry bubble columns and address issues related to scale-up. Experirimental investigations to examine the effect of operating conditions such as superficial gas vvelocity, solids loading, type of distributor etc. on the fluid dynamics are to be made. The speecific objectives that have been set out for the first year of the project are as follows :

1. Assess the suitability of avvailable experimental techniques for the measurement of global and some local hydrrodynamic parameters in an industrial scale system and make recommendations for tthe use of these techniques at La Porte.
2. Interpret the existing tracer c experiments and make recommendations for future tracer tests on La Porte reactor.
3. Modify the CARPT/CT expperimental facility for study of slurry bubble columns.
4. Develop a phenomenological l model for the key hydrodynamic features in bubble columns as a basis for an improved rereactor model.
5. Introduce appropriate closuure schemes and constitutive forms in the hydrodynamic codes to achieve agreements s between data and models and test model reliability.

The activities that have been unndertaken during the third quarter (September - December 1995) towards fulfilling the abovve mentioned objectives are described in the subsequent sections.

2 Review of Measuurement Methods

This study has been completed annd a summary of findings has been reported in the second quarterly report. A topical repoort on the subject entitled "Measurement Techniques for

Local and Global Hydrodynamic QuQuantities in Two and Three Phase Systems", has been submitted to Air Products.

3 Interpretation of Tracer Runs at La Porte

The reactor that was studied was thethe Alternative Fuels Development Unit (AFDU) at La Porte, Texas, which is a stainless ststeel bubble column reactor owned by D.O.E., with an internal diameter of 0.57 m and liqquid height of 7.62 m. The slurry phase was powdered catalyst suspended in hydrocarbon ı oil. Gas was distributed via a sparger. For the cases considered thus far, the reactor temmperature was 300° C, and pressure was 2.7 atm. The reaction was the dehydration of isobutanol to isobutylene and water. Due to complete conversion, the gas holdup was foundd to be almost doubled in the reactor.

Radioactive liquid and gas tracerr measurements were made in the reactor. Ar-41, which is soluble in the liquid phase, was usised as the gas phase tracer. Powdered manganese oxide was used as the liquid tracer since thethe particles were small enough to mimic the liquid flow. The distribution of the gas and liqquid tracers in the column was monitored by four rings of four evenly distributed scintillatidon detectors, with an extra set of detectors at two other levels to monitor the gas distributiorn.

Since the tracers are radioactive,e, the signals measured by the scintillation detectors are affected by the solid angle subtendeled at the cylindrical detector, the distance between the radiation source and the detector, aand other effects such as attenuation and buildup. These effects have been properly accounteed for, the details for which are presented in Toseland et al., (1995). The normalized tracer curve that is finally obtained is taken to be linearly dependent on the tracer concentratidon.

The standard dispersion model l was used to describe mixing in the liquid phase. For the gas phase, a dispersion model wwhich included the solubility of Argon tracer was considered. The following equations descriribe the gas and liquid mass balance for the tracer when interphase mass transfer resistance i is also considered:

$$D_G\frac{\partial^2 C_G}{\partial z^2} - \frac{UU_G}{\rho\rho_G}\frac{\partial C_G}{\partial z} + k_l a(HC_L - C_G) = \frac{\partial C_G}{\partial t} \tag{1}$$

$$D_L\frac{\partial^2 C_L}{\partial z^2} - \frac{\epsilon_G}{\epsilon_L}k_l a(HC_L - C_G) = \frac{\partial C_L}{\partial t} \tag{2}$$

The following boundary and inititial conditions were used :

$$t = = 0, \quad C_L = 0; \quad C_G = 0 \tag{3}$$

bubble size distribution at various flflow conditions.

(iv) Improved automatic calibraration for CARPT is progressing in parallel as part of DE-FG 22-95PC95212.

(v) The possibilities of obtaining both liquid and solid velocities via CARPT are currently being studied as part of this programm. If it proves feasible this will provide us with the needed information on solid-liquid slip veloocities.

Below we will briefly describe tlthe improved accuracy of CARPT obtained by wavelet filtering which is pertinent to this s project. The wavelet filtering technique removes the intrinsic white noise (due to fluctuatation in source emission) in the time versus instantaneous position data.

The statistical nature of the gaamma radiation emitted from the particle gives rise to noise in the radiation intensity data a and this gets transmitted to the position data. Wavelet analysis, a time-frequency based meethod, was identified as an appropriate method for analyzing the nonstationary and localizzed data arising from CARPT experiments in multiphase systems.

To demonstrate its suitability iin this regard, an experiment was conducted with a controlled motion of the radioactive tiracer particle. This enabled *a priori* knowledge of the trajectory of the particle and provivides a reference against which the results from CARPT experiments subject to wavelet pacicket filtering can be compared. A quantitative estimate of the errors involved in the estimnation of the particle position, as well as the extent to which the intrinsic noise in the datta is removed can therefore be arrived at. Thereafter the technique was applied to data fromn bubble column experiments.

4.1 Algorithm for filterring CARPT data using wavelet analysis

A brief outline of the algorithm usesed in the filtering procedure will be described here. For the sake of simplicity the mathemaatical details will be omitted. Wavelet packet decomposition using Daubechies' orthonormmal, nearly symmetric wavelets is employed for analysis. The algorithm consists of first trannsforming a set of data onto the wavelet packet domain, yielding a set of wavelet packet coeefficients that contain the time-frequency (scale) content of the original data. The best basisis representation of the coefficients is then obtained, by eliminating redundant coefficients.s. In the wavelet packet domain the coherent structures of the original signal are well repnresented by a few large coefficients while the incoherent part, that is basically the noise iin the signal, is in the form of a large number of small coefficients. The wavelet packet ccoefficients (wpc) are therefore arranged in descending order of energy (energy $E_{wpc} = wpc^2$). The first few significant coefficients correspond to the coherent part of the signal whhile the remaining weak coefficients depict the noise. The

coherent part is extracted by retaining the first few largest wavelet packet coefficients that possess an energy ($E_\epsilon = \epsilon E_S = = \sum_{i=1}^{I_\epsilon} wpc^2$) equivalent to a fraction ϵ of the total signal energy ($E_S = \sum_{i=1}^{N} wpc^2$). These ϵ coefficients are then re-ordered and reconstructed to yield the filtered signal. The weak coefficients (incoherent part) that remain are re-ordered and reconstructed to give the noise filtered. The tuning parameter in this algorithm is the energy threshold ϵ. This parameter is evaluated by conducting trial runs for a few data sets in the signal. Characteristics of white noise, such as the autocorrelation coefficient, are used as reference to select a proper threshold. Experiments show that the energy threshold is generally around $95-98\%$ of the total signal energy. It is found that the results are insensitive to minor variations in the threshold value. Filtering using the above algorithm ensures maximum extent of reduction of the noise in the data, resulting in a smoother version of the signal and retains the sharp features arising from the nature of the flow in the system.

In order to verify the applicability and effectiveness of the algorithm for filtering noise from the data, the algorithm was tested with data produced from experiments for a controlled motion of the tracer particle.

4.2 Experimental setup

The experimental setup principally consists of two motors, a screw conveyor and a plate as shown in Figure 4.1. Motor I I is secured at the bottom of the structure and is geared to a screw conveyor that is positioned vertically. The screw conveyor supports a vertical frame on top of which the plate is mounted. The shaft of motor II, which is fixed to the top of the plate, is connected to a smooth, circular disc. The radioactive particle to be tracked is fixed to the tip of a thin plexiglas rod attached to the disc. Operation of motor II causes the particle to move in a circular motion. The maximum frequency of motion is 3 Hz. The distance of the particle from the center of radius varies from 7 to 8 cm. Simultaneously motor I causes the plate held to the frame to move vertically in "up and down" motion (with frequencies of the order of 0.1 Hz). The maximum vertical distance traversed by the particle is 6.4 cm. By this arrangement the particle is made to move in a spiraling 3D motion, with high (3 Hz) and low (0.2 Hz) frequencies. The two motors are driven by microprocessors, which are interfaced with a personal computer. A trolley system with guiding wheels provided for guiding the frame helps in minimizing the vibration of the setup. Calibration is first done using various particle positions that cover the entire range of experimental runs. Subsequently the experimental runs are performed. In each run, the speed of the two motors is varied, thereby varying the velocity of the particle. Eight such runs were performed.

A summary of the results for the entire set of runs is presented in Table 4.1 which reports

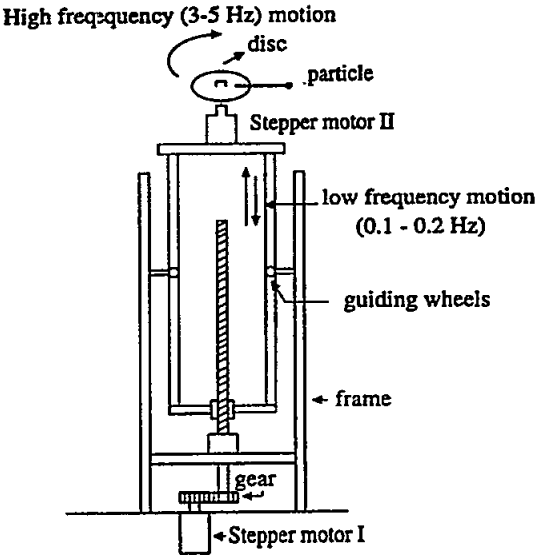

Figure 4.1 : Experimental setup for controlled motion of particle

the errors in position and spurious rrms velocities, before and after filtering. It is evident by examining the results, that there is s significant improvement in the accuracy of estimation of both the positions and velocities of f the moving particle. The residual error (spurious rms velocities) after filtering the data is 2-5 cm/sec. There is an average of 75% reduction in the level of noise in the data. With regaard to the magnitude of the rms fluctuating velocities of the liquid in bubble columns, which a are an order of magnitude higher, the reduction in error is considered substantial.

4.3 Results for bubble ccolumn experiment

We now show results for filtering of f the data from a bubble column experiment. The experimental conditions for the run consisidered are : column diameter 19.05 cm, superficial gas velocity 3.2 cm/sec and superficial liliquid velocity 0 cm/sec. The results presented in Figures 4.2, 4.3 and 4.4 are one dimensionalal profiles generated by averaging over the middle section of the column, where the flow is fullly developed. As expected, there is no appreciable difference between the filtered and originnal mean axial velocity profiles shown in Figure 4.2. This is because time averaging of the inststantaneous velocities, averages all the fluctuations in the data, including the inherent noise ddue to statistical fluctuations of the radiation. Figures 4.3 and 4.4 show the turbulent kinetic c energy and the Reynolds shear stress respectively. Here it can be seen that filtering has reeduced the magnitude of these parameters. The data is

Table 4.1. Errors in Estɜtimation of Particle Position (cm) and Velocity (cm/sec)

		error in position, cm				error in velocity, cm/sec	
		Before e Filtering		After Filtering		Before filtering	After Filtering
Run No.	Direction	rms	ɜ min/max	rms	min/max	rms	rms
Run 1	x	0.32	- -1.17,1.12	0.19	-0.7,0.6	20.5	4.16
	y	0.36	-.15, 1.2	0.26	-0.75, 0.8	20.01	4.66
	z	0.49	-1.7,1.4	0.25	-0.7,0.74	30.36	1.68
Run 2	x	0.30	- -1.23, 1.25	0.2	-0.76, 0.64	21.0	5.6
	y	0.33	- -1.43, 1.34	0.22	-0.79, 0.86	19.4	5.7
	z	0.49	-1.6,1.6	0.2	-0.67,0.8	29.6	1.6
Run 3	x	0.32	- -1.16,1.13	0.21	-0.7,0.9	19.3	3.2
	y	0.31	-1.2,1.2	0.21	-0.85,0.8	18.0	3.6
	z	0.47	- -1.5, 1.75	0.17	-0.9, 0.6	28.9	1.34
Run 4	x	0.32	- -1.08,1.12	0.22	-0.75,0.86	19.5	4.8
	y	0.32	-1.5,1.25	0.23	-0.7,0.75	19.0	4.5
	z	0.46	-1.4,1.4	0.21	-0.65,0.61	29.0	1.38
Run 5	x	0.3	- -1.11,1.32	0.19	-0.9,0.66	20.2	5.4
	y	0.29	-0.89,0.9	0.16	-0.61,0.65	18.7	3.8
	z	0.47	-1.6,1.4	0.22	-0.87,0.72	29.2	1.56
Run 6	x	0.32	- -1.36,1.08	0.19	-0.55,0.52	20.9	6.3
	y	0.29	-1.4,1.0	0.17	-0.68,0.7	19.11	3.4
	z	0.39	- -1.42, 1.45	0.14	-0.64,0.32	26.1	1.01
Run 7	x	0.31	- -1.16,1.08	0.21	-0.8,1.0	19.78	4.18
	y	0.28	- -1.14,1.11	0.14	-0.84, 0.82	18.69	3.51
	z	0.37	- -1.09,1.21	0.20	-0.86, 0.72	25.73	1.48
Run 8	x	0.31	- -0.97,1.03	0.03	-0.04,0.03	16.99	0.07
	y	0.28	- -1.10,1.15	0.007	-0.01, 0.02	17.94	0.04
	z	0.40	-1.3,1.03	0.25	-0.79, 0.5	24.29	1.05

averaged over the middle section of t the column where there appears to be negligible axial dependence of the parameters, and v values are axially uniform. The profiles shown suggest that there is maximum turbulent shear and turbulent energy near the region of reversal in the flow direction. Comparison of these results for turbulent shear stress with data of Menzel et al. (1990), who used hot wire anemometry for measurement of the hydrodynamics, are shown in Figure 4.5. A good order of magnitude agreement is seen, which serves as an indirect verification of the results from CARPT for the turbulence parameters.

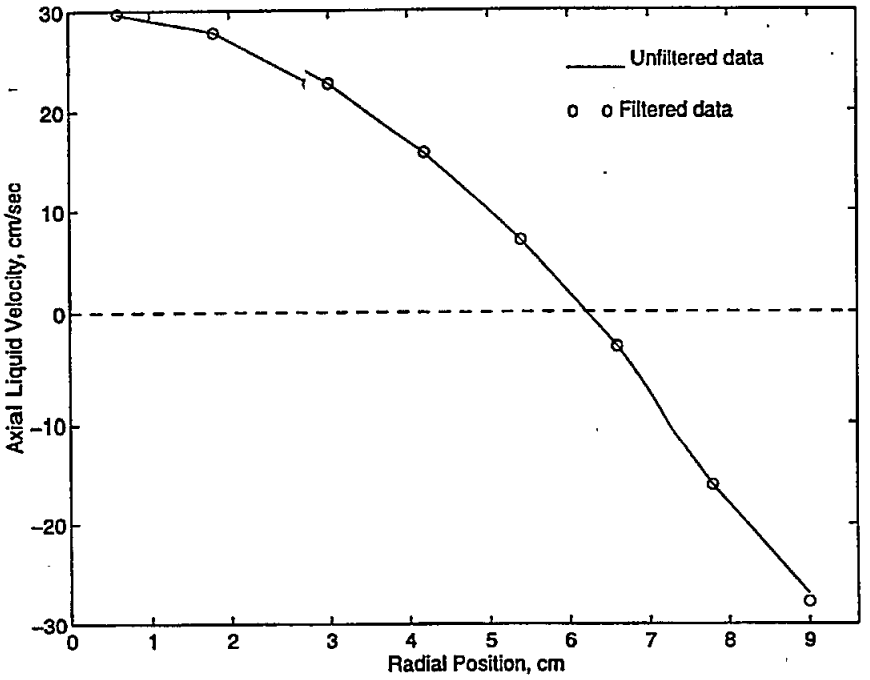

Figure 4.2 : One dimensional mean axial liquid velocity for an 8″ column, U_G 3.2 cm/sec

5 Phenomenological Model for Liquid Recirculation

The axial dispersion model (ADM) has been used in the past to fit the tracer response of multiphase reactors like bubble columns. In contrast to the computational fluid dynamics approach, which is directed at solving the complete transport problem in such reactors spatially and temporally, and involves massive computational power and problems of closure in the governing equations; phenomenological models are meant to be relatively simple, using a minimum number of adjustable parameters, and capture the essential features of the physics behind the backmixing in the system.

Models like the ADM and the tanks-in-series model are widely used in describing the mixing in flow systems, but are not found to be adequate in many instances, owing to the

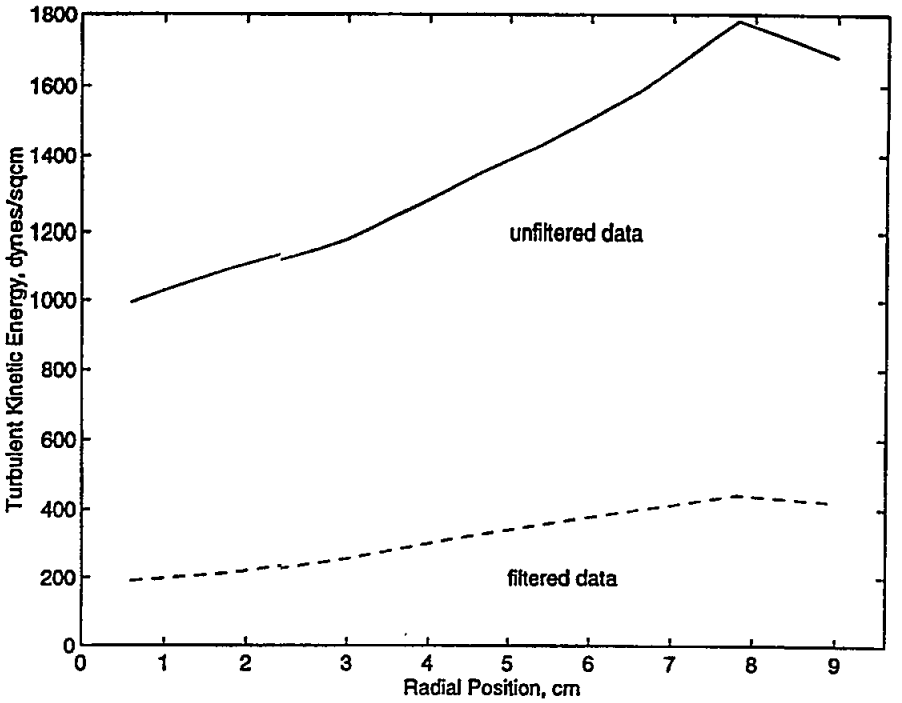

Figure 4.3 : One dimensional turrbulent kinetic energy for an 8″ column, U_G 3.2 cm/sec

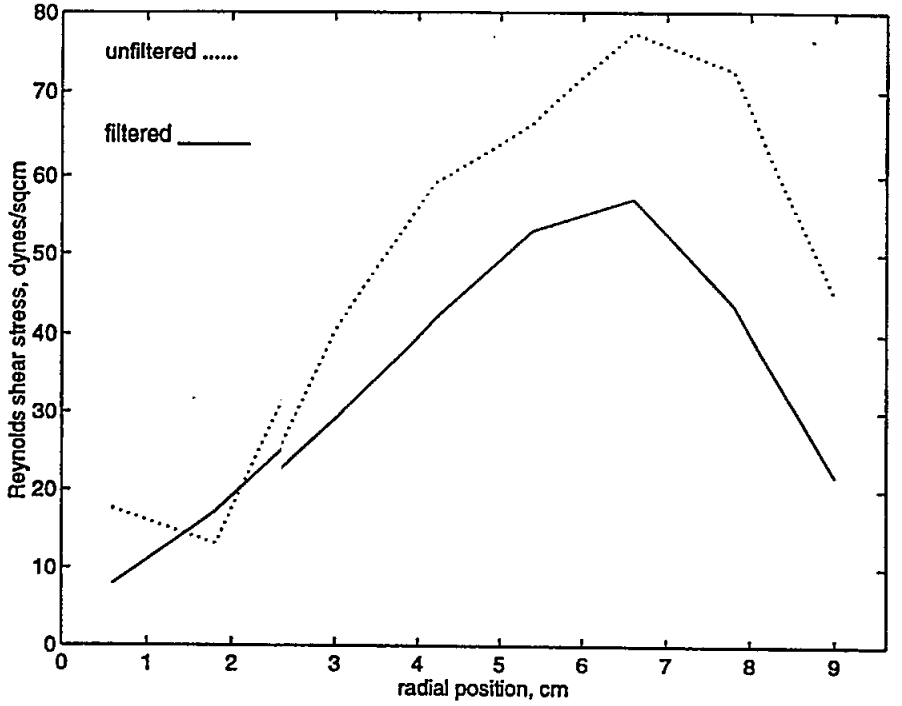

Figure 4.4 : One dimensional Reyrnolds shear stress for an 8″ column, U_G 3.2 cm/sec

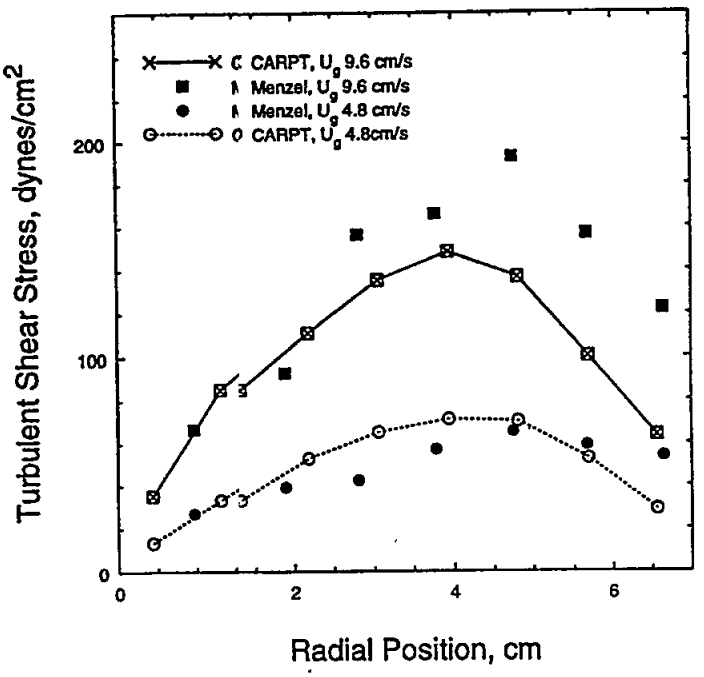

Figure 4.5 : Comparison of Experimental data for Turbulent Shear Stress from CARPT with Data of Menzel (Col. Dia. 14 cm)

fact that they describe mixing superimposed on unidirectional convective flow. It is well recognized however (Hills, 1974; Devannathan et al., 1990) that in bubble columns there is both upflow of liquid (cocurrent with gas), as well as downflow of liquid (countercurrent with gas). Further, there is vigorous lateral mixing as well, in columns operating in the churn turbulent regime. Clearly then, it is not surprising that the ADM fails in many cases in describing the liquid mixing pattern. Notwithstanding such inadequacies in the model however, it continues to be extremely popular both in academia and the industry essentially because it is computationally simple with only one fitting parameter, and also because resolving the spatial dimensions further demands measuring mixing parameters experimentally, an undesirable alternative.

At CREL, the CARPT-CT facility allows us to measure the time-averaged liquid velocity profile, the backmixing parameters and the time-averaged gas-holdup distribution in the system. It was felt that this experimental knowledge could be used to overcome the inadequacies in previous models, such as the ADM, as pointed out above.

5.1 Model developmennt:

In the proposed model referred to aas the Recycle-Crossmixing with Dispersion Model (RCFDM), the bubble column is divided axiaially into three sections, a middle zone and two end zones in which the liquid turns around ((Fig. 5.1). The end zones are considered to be completely mixed, because it is not possible ɜ to resolve the complicated hydrodynamics in this region using a one-dimensional model. TThe middle zone is divided into two sections, one with the liquid flowing up in the core regioion, and another with liquid flowing down at the walls. In

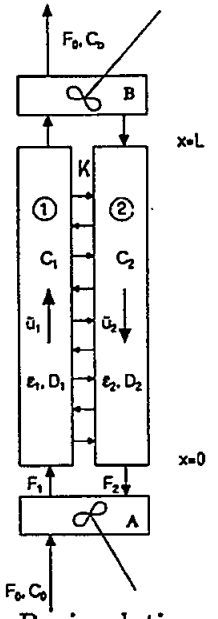

Figure 5.1: Schematic Diagram fofor Recirculation and Cross Flow with Dispersion (RCFD) Model

this way the radial variation of liqquid flow is lumped into two parts. The flow within each of these sections is considered ɪo be ɜ in the middle region of the bubble column where the flow is assumed to be fully developed ((an assumption based on the experimental observations of the liquid flow patterns obtained ɨ from CARPT in our laboratory).

Superimposed on the convectiɪve recirculation is the mixing caused by random turbulent fluctuating motion of the fluid elelements, caused by the wakes of the rising bubbles, which give rise to axial dispersion as welell as radial exchange between the two sections. Turbulent axial mixing is accounted for by ɾ an axial dispersion coefficient in each section, and radial mixing is incorporated by an exclhange coefficient between section 1 and section 2.

Based on the above assumptiɑions, the model equations may be formulated as follows.
For the upflow region:

$$\frac{\partial C_1}{\partial t} = 1 D_1 \frac{\partial^2 C_1}{\partial x^2} - \bar{u}_1 \frac{\partial C_1}{\partial x} - \frac{K}{A_1}(C_1 - C_2) \qquad (6)$$

where K is the exchange coefficieient (cm^2/s) between the upflow and downflow sections, D_1 is the dispersion coefficient in the upflow region (section 1) based on the liquid covered cross-sectional area, and, ϵ_1, $\bar{u_1}$, and A_1 are the average liquid holdup, velocity and cross sectional area of the upflow section. .

Similarly, for the downflow region:

$$\frac{\partial C_2}{\partial t} = D_2 \frac{\partial^2 C_2}{\partial x^2} + \bar{u}_2 \frac{\partial C_1}{\partial x} + \frac{K}{A_2}(C_1 - C_2) \tag{7}$$

The equations for the well mixed regions, A and B which are assumed to connect the ends of the recirculating sections, are, respectively:

$$V_a \bar{\epsilon}_a \frac{\partial C_a}{\partial t} = F_0 C_0 - F_1 C_a + F_2 C_2|_{x=0} \tag{8}$$

$$V_b \bar{\epsilon}_b \frac{\partial C_b}{\partial t} = F_1 C_1|_{x=L} - F_2 C_b - F_0 C_b \tag{9}$$

where F_0 is the inlet liquid volumetric flowrate to the column, F_1, F_2, F_a and F_b are the liquid volumetric flowrates in the upflow section 1, downflow section 2, region A and region B respectively. Initial conditions for a step input of tracer at the bottom of the column are:

$$C_0 = H(t) \quad and \quad C_1 = C_2 = C_a = C_b = 0 \quad @t = 0 \tag{10}$$

Boundary conditions for the upflow region are given by equations (6) and (7) and for the downflow region by equations (8) and (9), as follows.

For the upflow section:

$$\frac{\bar{\epsilon}_a}{\bar{\epsilon}_1} \bar{u}_1 C_a = \bar{u}_1 C_1|_{x=0} - D_1 \frac{\partial C_1}{\partial x}|_{x=0} \tag{11}$$

$$\frac{\partial C_1}{\partial x}|_{x=L} = 0 \tag{12}$$

For the downflow section;

$$\frac{\bar{\epsilon}_b}{\bar{\epsilon}_2} \bar{u}_2 C_b = \bar{u}_2 C_1|_{x=L} + D_2 \frac{\partial C_2}{\partial x}|_{x=L} \tag{13}$$

$$\frac{\partial C_2}{\partial x}|_{x=0} = 0 \tag{14}$$

The above model requires as inputs the input function of tracer, the dimensions of the column (Table 5.1), the average upflow and downflow liquid interstitial velocities, and the average holdups in the different sections of the column.

Table 5.1 Operatating Conditions for Tracer Experiments

Diameter of Column	19.0 cm
Height of Column	2.44 m
Sup. Gas Velocity U_g	10.0 cm/s
Sup. Liquid Velocity U_l	1.0 cm/s
Mean Residence Time of Liquid	3.25 min
Mean upflow velocity, $\bar{u}_1^*$	12.5 cm/s
Mean downflow velocity, $\bar{u}_2^*$	7.7 cm/s
Mean liquid holdup in upleg $\bar{\epsilon}_1^+$	0.792
Mean liquid holdup in downleg $\bar{\epsilon}_2^+$	0.88

* Ref. Fig. 5.2(a), + Ref. Fig. 5.2(b)

The experimental information was obtained from the CARPT-CT facility, from which the mean liquid velocities are calculated from the cross-sectional averaging of the recirculating liquid velocity profile (CARPT) (Fig. 5.2(a)) and the holdup profiles (CT) (Fig. 5.2(b)).

The model equations were solved numerically using implicit finite differences with backward differences in spatial coordinates. Implicit method was necessary because of the nature of the boundary conditions, and appropriate discretization was required for accurate convergent results. Solution of the model equations results in the F-curve, which on differentiation yields the E-curve.

The heights of the two well-mixed regions A and B are assumed to be equal to the diameter of the column, an assumption based on observation of churn-turbulent bubble columns. However, it was found on running the simulation that the model is insensitive to the volumes of these sections.

5.2 Results and discussion:

The objectives in developing this model were twofold: first, we wanted to develop a model which, based on the physics, would in general perform better for churn-turbulent bubble columns than existing models. Secondly, we wanted to see if given the experimental observations from CARPT-CT, whether it would be possible to predict the RTD to a reasonable extent.

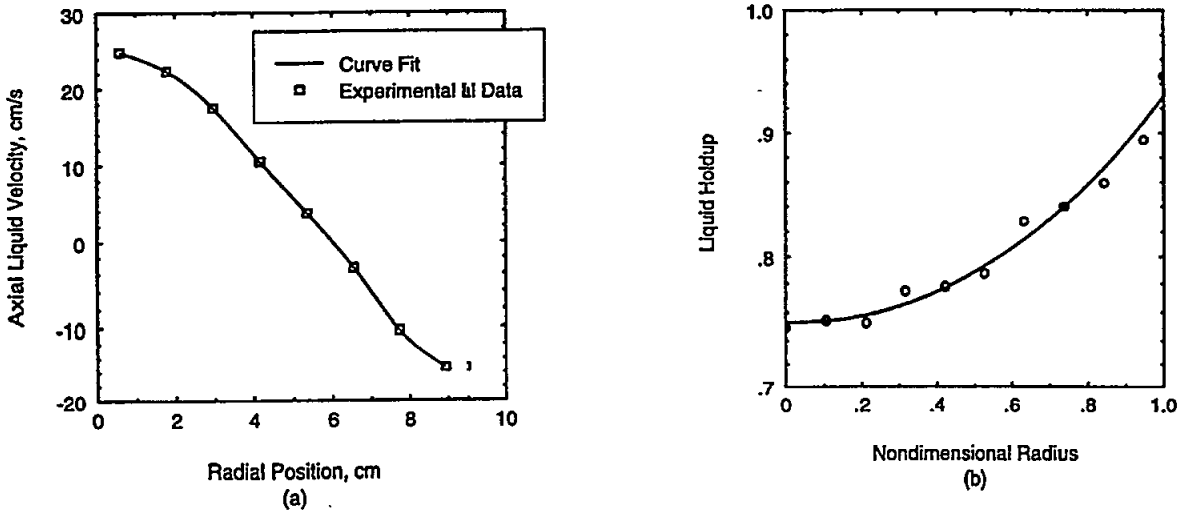

Figure 5.2: Azimuthally, Axially and Time Averaged (a) Liquid Axial Velocity Profile, (b) Liquid Holdup Profiles

As a comparison of the models, the ADM, the recycle with crossmixing and the present model (RCFDM) were used to fit the experimental data (Fig. 5.3).

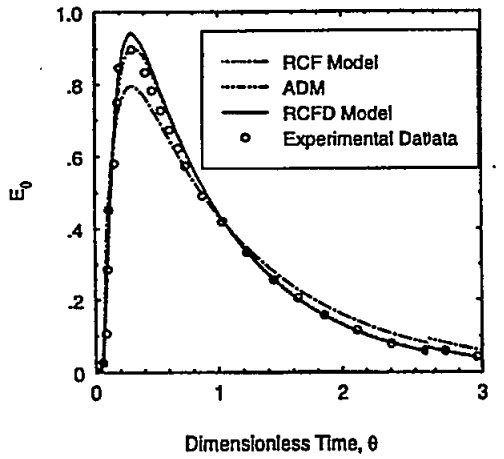

Figure 5.3: Measured RTD of an Experimental Bubble Column versus Model Predictions

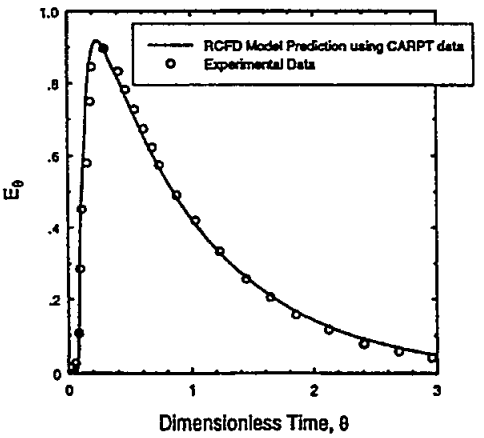

Figure 5.4: RCFD Model Predictions Based on Parameters Estimated from CARPT Data

The model parameters thus obtained in each case are shown in Table 5.2. Also shown is the sum of square of errors, which is found to be minimum in the present case.

An independent assessment of the model parameters was attempted using the experimental data from CARPT. From CARPT, an estimate of the axial dispersion coefficients can be obtained by spatial averaging of the measured axial eddy diffusivities in the upflow and downflow sections, respectively. The average value of the radial eddy diffusivity at the

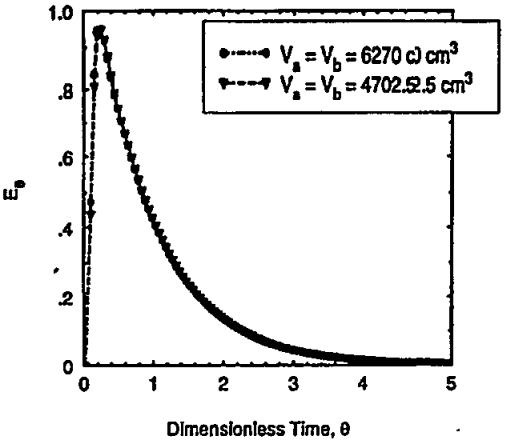

Figure 5.5: Effect of Entry and Exitit CSTR Volumes on Prediction of RCFD MModel

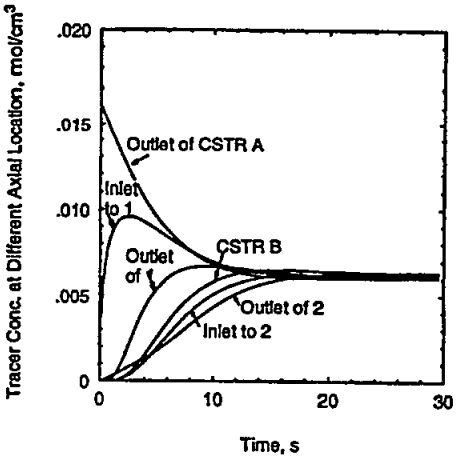

Figure 5.6: RCFD Model Prediction of Response to an Impulse Injection (D = 19 cm, U_g = 2cm/s, U_l = 0 cm/s)

Table 5.2 Model Parameeters and Sum of Square of Errors for Models

Model	Fitted/Predicted* Parameter	e^2
RCFDM	$D_1{}_1 = 113\,cm^2/s, D_1 = 113\,cm^2/s,\ k = 69\,cm^2/s$	0.0366
ADM	$D_{eff} = 257.5\,cm^2/s$	0.0403
Recycle-Crossflow	$k = 30.37\,cm^2/s$	0.132
RCFDM from CARPT*	$D_1 = 2285\,cm^2/s, D_1 = 440\,cm^2/s,\ k = D_{rr_o} = 43\,cm^2/s$	0.0724

point of inversion is taken as the crcrossmixing coefficients between the two legs. The RCFDM prediction using these parameters ŧ (Table 5.2) is shown in Fig. 5.4. This exercise seems to predict the tracer response indepenndent of any experiment, based on the knowledge from the hydrodynamics.

Figure 5.5 shows that changing ʒ the volumes of the inlet and exit well mixed zones has no appreciable effects on the predicteed tracer response. However, including them in the model renders the computations stable annd does not lead to sharp fronts at the inlet and exit.

Since the RCFDM, using paranmeters estimated from CARPT results, is able to match well the observed tracer response ((Fig. 5.4), we proceed to study the mixing behavior for batch liquid, in a 19 cm diameter c column of expanded liquid height 65 cm, at a superficial gas velocity $U_g = 2cm/s$. A pulse ɨ injection into the region A is simulated, using the batch version of the RCFDM. Figure 5.66 shows the resulting tracer concentrations as a function of time, at different axial locationns in the column. As expected from the physics of the

problem, there are instants of offshoots s in the upflow section of the column where the tracer moves up initially by convection. Although these predictions look quite realistic, they need to be confirmed by additional tracer experiments. Needless to say, ADM or any other one dimensional model cannot predict such a variation in the dynamics in different parts of the system.

5.3 Future work:

The lack of fully quantitative agreement between the RCFDM and CARPT data can be attributed to the fact that as it currently stands, the model does not consider the radial variation of liquid velocity and holdup profiles, but takes into account only the average flow in each section. Hence, the axial dispersion coefficient in each section does not directly correspond to the axial eddy diffusivities but also accounts for the contribution from the radial variation of axial liquid velocity. The relationship between CARPT measurements and the RCFDM parameters need to be further developed based on additional analysis, which is in progress.

One needs to develop some independent means of predicting at least the average upflow and downflow velocities either through theory or through simple experiments, because one cannot be expected to make CARPT runs at all industrial setups for which the use of the RCFDM is intended.

The model will be modified for predicting the tracer response of reacting systems in which gas may be evolved, causing a significant axial variation in holdup because of reaction (such as in the runs made at AFDU, La Porte, Texas). For this the equations have to be modified

for predicting the response of radioactive tracer through detectors placed at the wall (since each detector spans a solid angle).).

Finally, the expressions for interphase mass transfer will be incorporated into the model to incorporate the effect of soluble gas. The ultimate idea should be to develop a single physics-based phenomenological model which is able to predict the response of both gas and liquid phase tracer.

6 CFDLIB Codes and Simulation

The Computational Fluid Dynamics Library (CFDLIB) code was developed at Los Alamos National Laboratory (LANL) under a CRADA agreement between Amoco Oil R & D and LANL. Being a sponsor of the Chemical Reaction Engineering Laboratory (CREL), Amoco granted CREL the privileges of using the CFDLIB code. The CFDLIB codes are capable of simulating three dimensional, multiphase, multispecies flows. Possibilities for including chemical reactions exist.

Here we report a test case for a gas-liquid flow problem that has been simulated. For this simulation the experimental conditions of Chen et. al. (1989) were considered. In their experiments the gas-liquid flow in a two dimensional bubble column was studied using flow visualization techniques. The experiment was conducted at several L/D ratios of the dispersion and in all the cases Chen et. al. (1989) observed the formation of a series of well defined counter rotating circulation cells in the flow. The geometry simulated is a two dimensional bubble column with a width of 11 cm and three of the L/D ratios used by Chen et. al. were simulated. The superficial gas velocity was 0.035 m/s. Figure 6.1 shows the computed flow fields at one instant of time (approximately 90 seconds after start up) and it can be seen that the code is able to predict the experimentally observed circulation cells at all the three L/D ratios. The most important factor in the simulation of multiphase flow using a CFD code is in the choice of the interfacial momentum exchange terms. For this particular simulation the effects of drag, lift and virtual mass were used. The turbulence effects were modeled using the mixing length approach. The models for closure of these terms were as follows:

- Drag is expressed as

$$\theta_k \theta_l \frac{\rho_c}{\theta_c} \frac{3}{4} C_D \frac{|U_{rel}|}{d_p}$$

- Virtual mass effects are expressed by

$$\theta_d C_a \rho \frac{D(u_k - u_l)}{Dt}$$

- Mixing length model is used fofor turbulence closure

$$< \theta_l \theta_k \rho_o u_k' u_k' > = -\rho l^2 (\nabla \cdot u_k)^2$$

A constant bubble size was useed in the simulation and the value of C_D was set to 0.44 since the particle Reynolds number r turns out to be in the inertial range. C_a - the coefficient in the virtual mass model was set t to the standard value of 0.5. The mixing length scale was set to 1.5 cm and this value wavas arrived by trial and error based on the observed flow pattern.

Currently, the code is being benmchmarked against a wide range of multiphase flow problems for which experimental or simmulated results are available in the literature. Specifically efforts are being directed towards ggas-liquid flow systems (bubble columns) under operating conditions for which experimental r results have been obtained using the CARPT-CT system in our laboratory.

7 References

Chen, J. J. J., Jamialahmadi, M. anand Li, S. M., 1989, Effect of Liquid Depth on Circulation in Bubble Columns, Chem. Eng. RRes. Des., Vol. 67, pp. 203-207.

Devanathan, N., Moslemian, D. a and Dudukovi\'c, M. P., 1990, Flow mapping in bubble columns using CARPT, Chem. Enngng. Sci., 45, 2285.

Hills, J. H., 1974, Radial nonuniforrmity of velocity and voidage in a bubble column, Trans. Inst. Chem. Engng. 52, 1-9.

Menzel, T., T. in der Weide, O. Staudacher, O. Wein and U. Onken, 'Reynolds Shear Stress for Modeling of Bubble Column Reactors', Ind. Eng. Chem. Res., Vol. 29, 988-994 (1990).

Toseland, B. A., Brown, D. M., Zoou, B. S. and Dudukovi\'c, 'Flow Patterns in a Slurry Bubble Column Reactor under Reaction CConditions', Trans. I. Chem. E., 73(A), 297 - 301.

Figure 6.1: Simulation of flow patte n a two dimensional bubble column

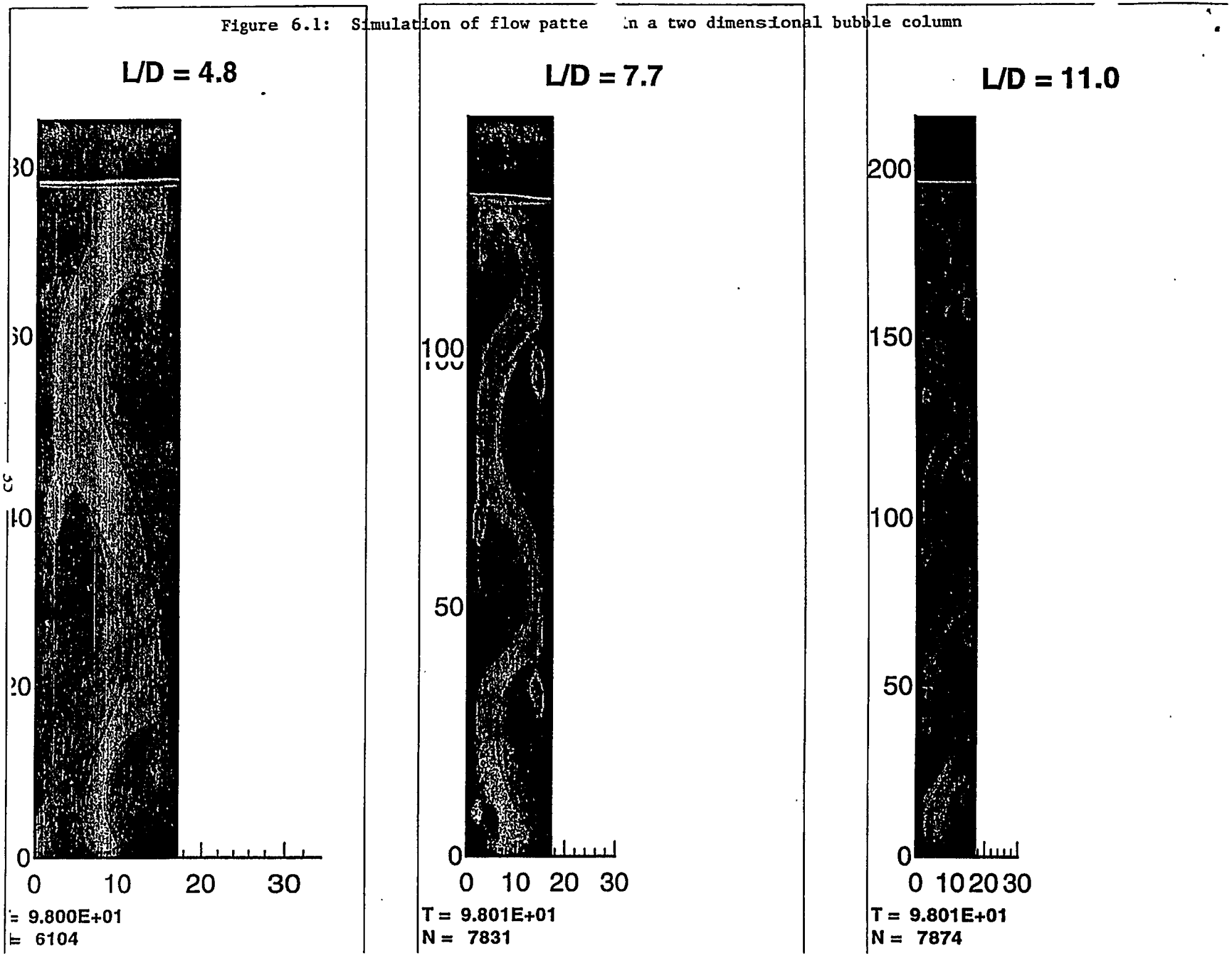

Task 4/Task 6 Data Processing for SCBR Tracer Runs

Tracer Studies

Introduction

As discussed in the last quarterly report[1] a series of tracer studies has been carried out using the DOE AFDU at LaPorte. This section describes the results of the most recent (June 1995) tracer studies. The results are presented in the form of graphs which illustrate the resolution of the various issues in the trial. A more quantitative report will be written when the mathematical analysis of the residence time distribution studies is completed at Washington University.

Plant Trial Results

Planning for the trial was discussed in the last report. A series of technique improvements and operating procedures was proposed for the trial based on our previous experience. These issues are discussed below:

a. Calibration

Seven rings of four detectors were placed on the column. The previous practice was to calibrate the detectors to each other, detector ring by detector ring. No attempt was made to relate the calibration for one ring to that of the another. We requested that all detectors be calibrated on the ground. Unfortunately, for the present time, the results were reported based on the old calibration method. A calibration chart is available for each detector so that the values can be readjusted at a later date. A potential issue is that the response of a detector is related to the length of electric cable attached. Thus, the best calibration results when the detector-cable pair are calibrated together. This will be requested next trial. An example of the problem caused by ring-by-ring post- calibration is shown in Figures 1 and 2.

Aside from the differences caused by the changes in holdup with height, the radiation level in the column should be equal, and all of these traces should converge to a single point for long periods. As shown in Figure 1, the final intensity varies over the height of the column. This variation is apparently not correlated to height or holdup profile. As shown in Figure 2, all of the data converge for a single ring, but the intensity differs greatly for even adjacent rings. As indicated above, the calibration data for each detector exists and, thus, a first-order correction can be made when the calibration factors are obtained from Tracerco.

[1]Engineering Development of Slurry-Bubble-Column Reactor (SCBR) Technology

Figure 1
Intensity) Proceeding Up South Side of Reactor

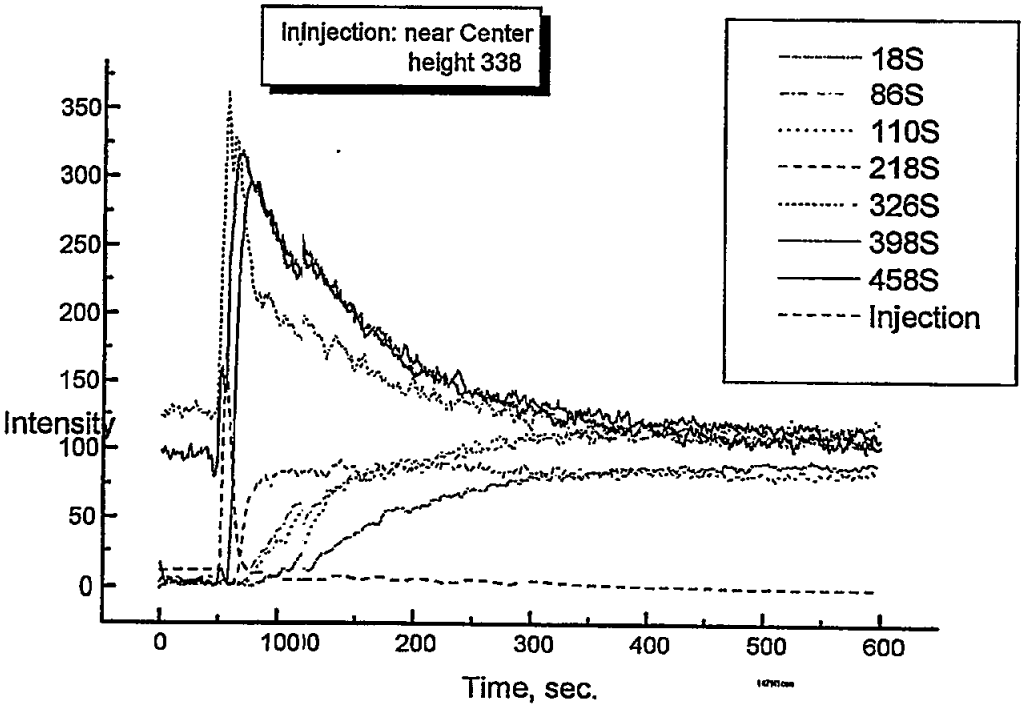

Figure 2
Intensity for Two Consecutive Rings of Detectors

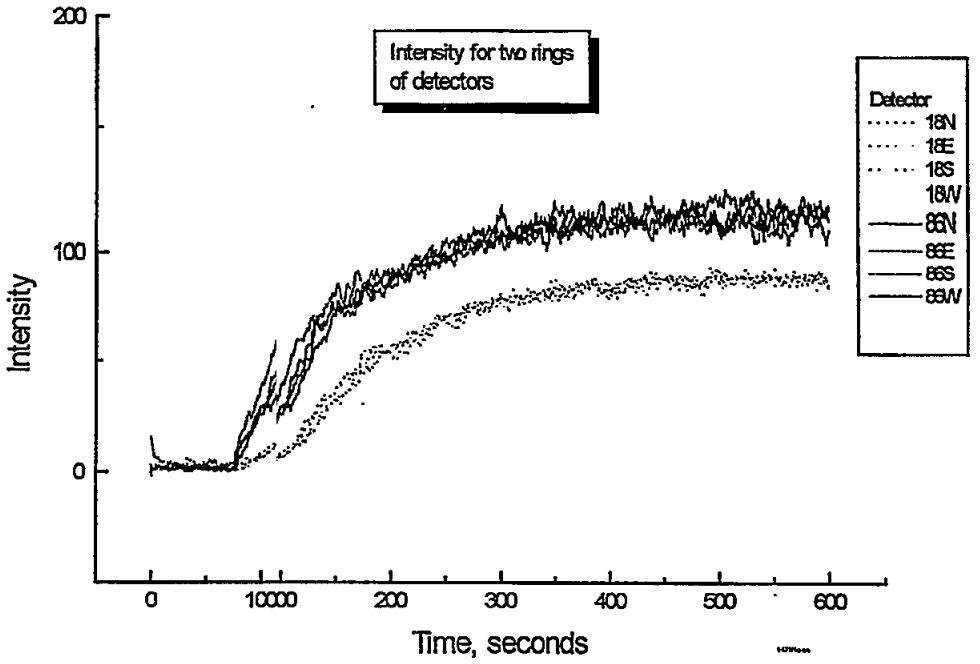

b. Gas Recycle

Some unreacted syngas is recycled to the reactor. The recycle stream will contain some of the tracer gas and, thus, cause a second pulse through the column. Preliminary calculations indicated that the residence time in the recycle loop should be 5-10 minutes. It was judged that the system would have returned to baseline by this time so that the recycle should not affect the initial residence time distribution (RTD) measurements.

As shown in Figure 3, a second peak is seen starting at about 5 minutes after the initial injection. The original radiation pulse shows a return to baseline, confirming the judgment made in the planning process that the recycle would not affect the RTD measurements. The peak is long and extends over a long period, indicating that there is extensive mixing in the recycle section as anticipated.

Figure 3
Typical Gas Phase Profiles

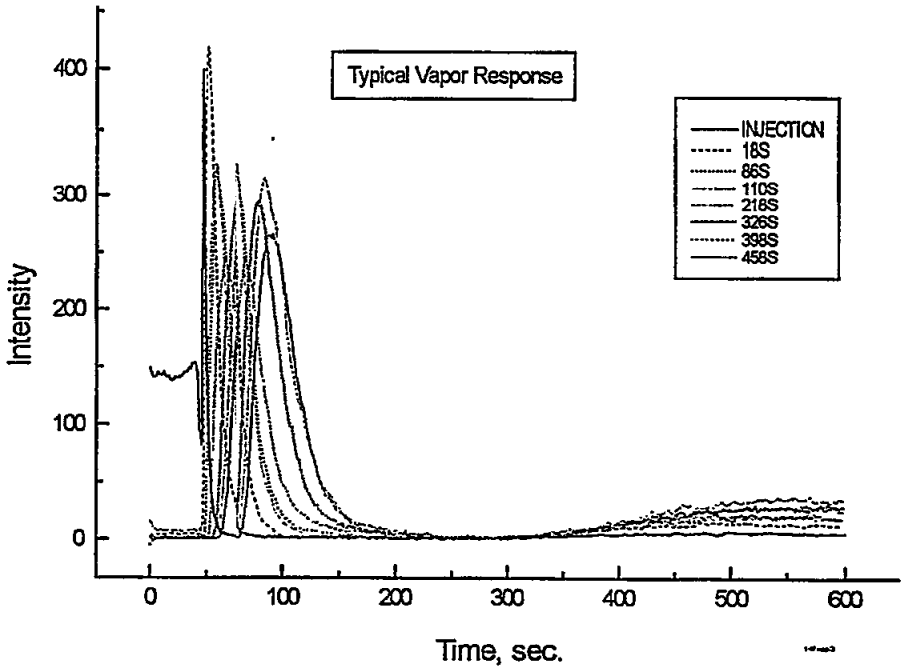

c. Liquid Phase Profiles

Typical radiation profiles for an injejection at the side of the column are shown in Figures 4 and 5. Figure 6 shows a typical response fi for an injection in the center of the column.

Figure 4
Liquid Phaase Profiles-High Side Injector Height

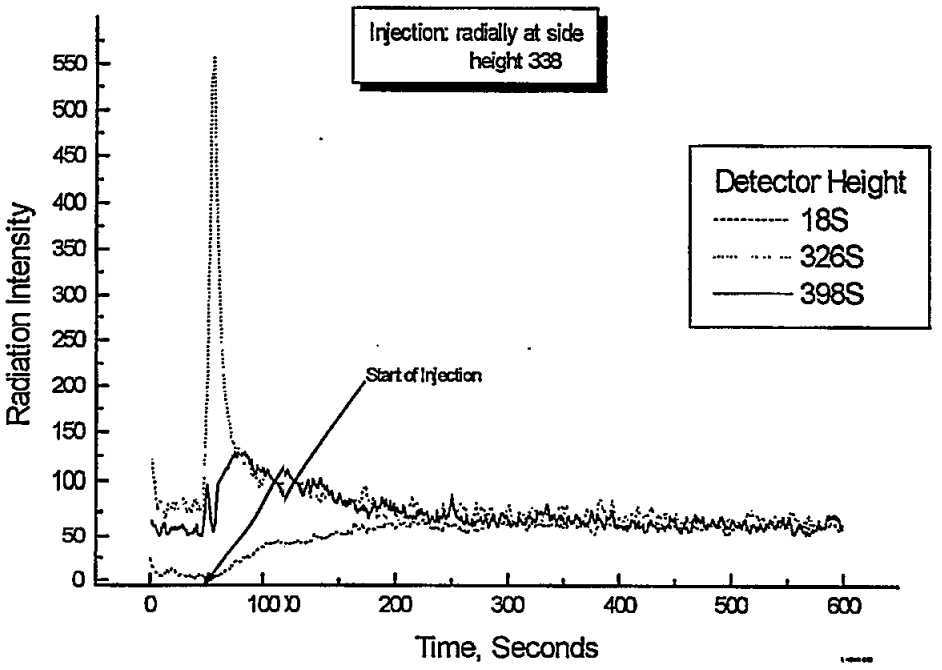

Figure 5
Liquid Phase Profiles- Side Injection, Lower Nozzle

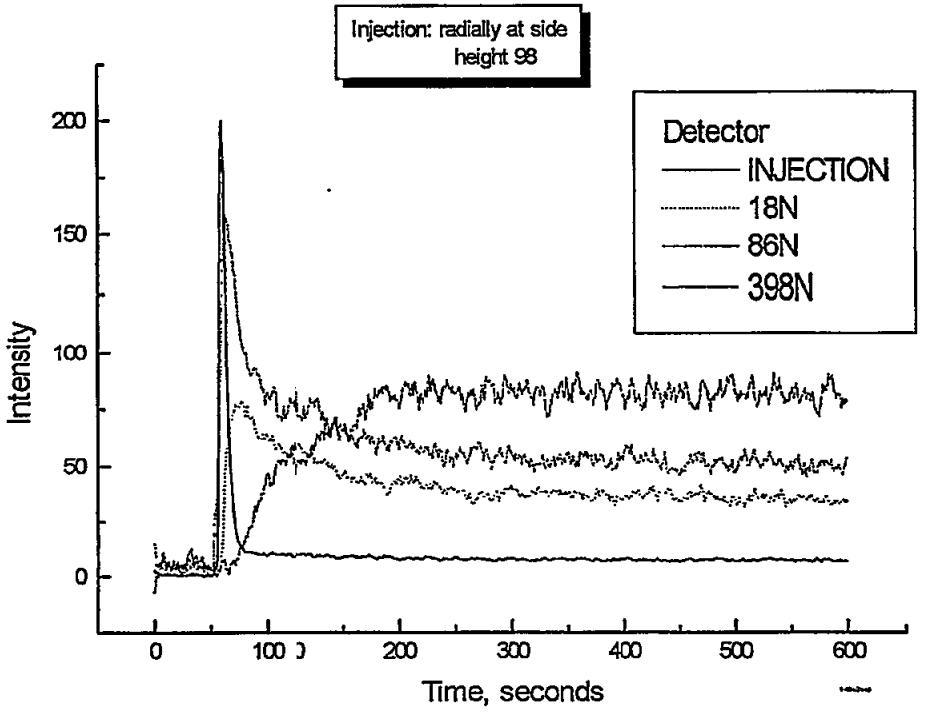

Figure 6
Liquid Phasse Profiles- Low Center Injector Height

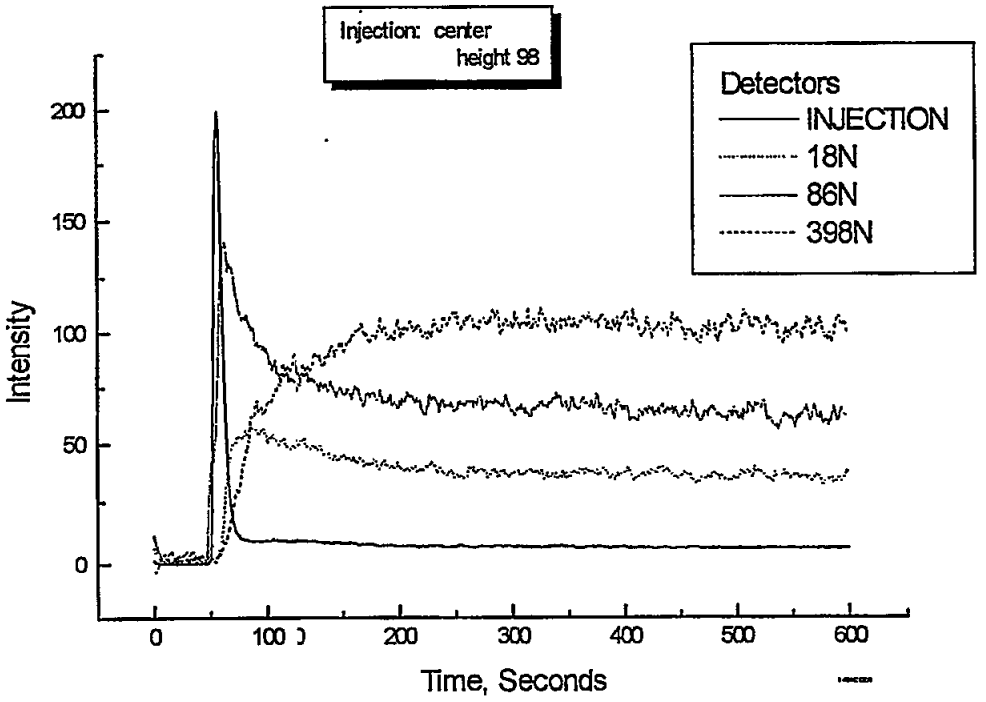

Standard profiles which one would d expect from an axial dispersion model are developed far away from the injector-for the detector atıt 18 for the high injection(338) and for the detector at 398 for the low injection(98). However, thehe profiles near the injection point are distorted by time-averaged motion of the eddies in thehe column. Further evidence of the time averaged convective motion can be seen in Figures 7 and d 8.

Figure 7
UUpward Flow at the Center

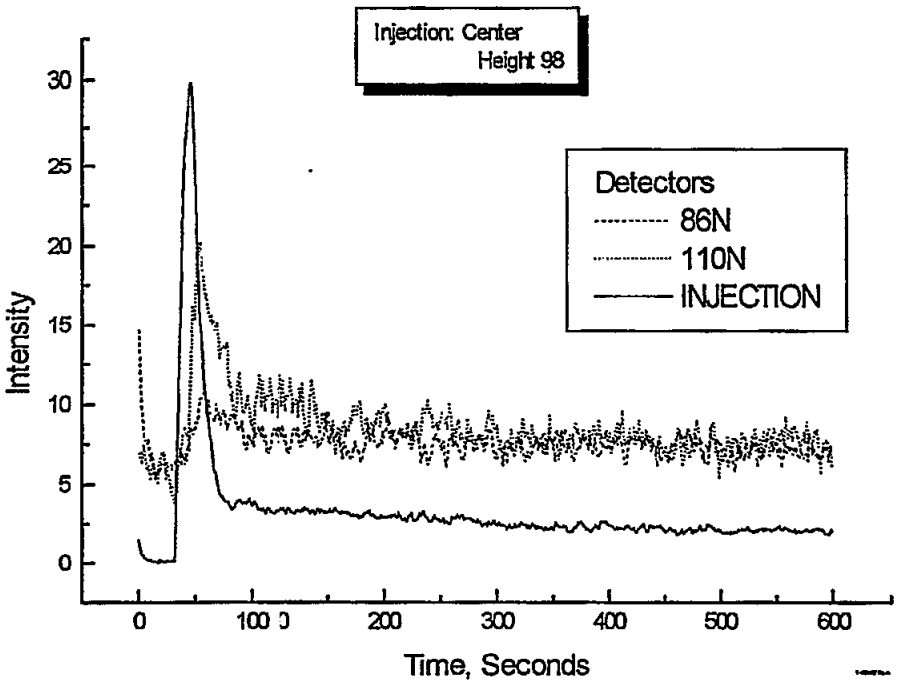

The detectors immediately above and below the injection point show a sharp spike of radiation immediately after injection. This is s an indication that part of the injection is swept upward by upflowing eddy, while part is swept it downward by a downflowing eddy. Note that the upflow pulse is much stronger, as would be e expected for the central region where the time-averaged flow is upward.

The time-averaged flow at the wall i is downward. As can be seen from Figure 4, there is a strong pulse down the column for the side e injection, indicating the predominance of average down flow at the wall. Only a small amount of f material travels up the column, in this case where the tracer is injected at the side of the column. I It should be noted that the injectors were fixed to inject horizontally at the wall, not downward as in the previous trial. Thus, we conclude that the tracer experiment provides good evidence e of strong downflow at the wall.

Since there is strong turbulence in thhe process, sometimes the flow can be seen to be almost evenly split in the pulse up and dowwn the column. This is shown in Figure 8 for a center injection. However, for most liquid tracer runsns, the predominant flow is up in the center and down at the wall. This means that the standard c one-dimensional dispersion model is not physically based for bubble column flow. Lack of a physsical basis implies poor scaleup capability. A new model is being developed by Professor Dudukkovic's group at Washington University.

Figure 8
Liquid Upflow and Downflow at the Injection Point

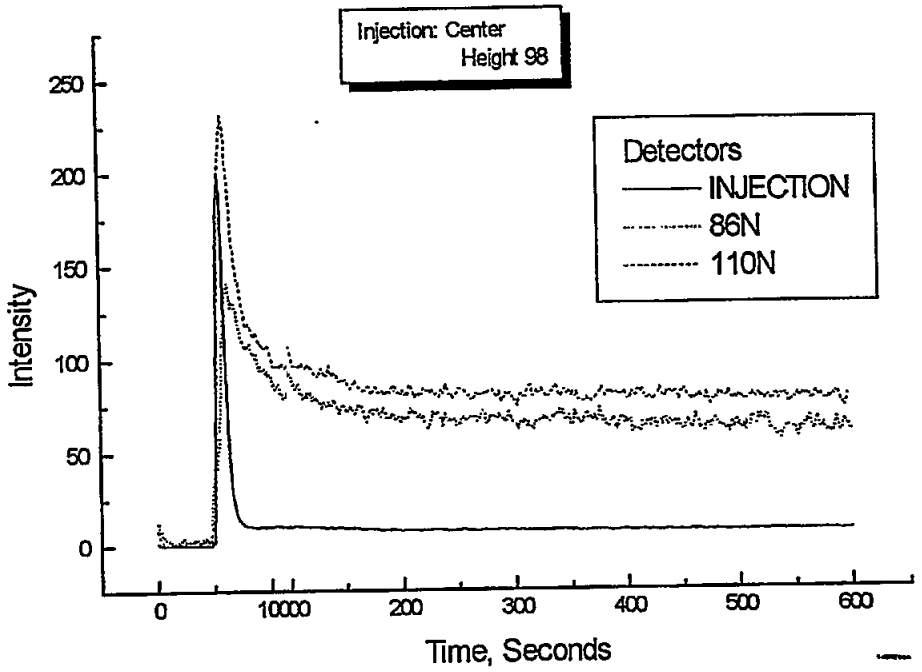

d. Gas Phase Tracer Results

Gas phase results look good. Typipical gas phase profiles have been shown in Figure 3. Gas phase results appear the same as for previvious trials.

A good, sharp initial pulse was obbtained. The profiles widen as the radiation pulse moves up the column. A substantial part of the v widening takes place before the first set of rings. As in the last tracer study, this is attributed to scsome CSTR-like mechanism in the very bottom of the column.

The time-of-arrival of centroid of t the pulse increases as it moves up the column. The time-of-arrival of the centroid is longer thaan that expected from a calculation based on the average superficial gas velocity (calculated d as $t = U_g/\varepsilon g$, where U_g is the superficial gas velocity and ε is the void fraction). As in the previvious tracer study, this is attributed to the solubility of the tracer gas in the process fluid, causing a a delay in the time of arrival. Thus, we anticipate that a version of the axial dispersion model that ε accounts for gas solubility will have to be used for analysis.